AIAA JOURNAL
Vol. 31, No. 9, September 1993

Exact Solutions for Static Analysis of Intelligent Structures

M. C. Ray,* R. Bhattacharya,† and B. Samanta†
Indian Institute of Technology, Kharagpur 721302, India

Exact solutions for static analysis of simply supported rectangular plate-type intelligent structures are presented. The intelligent structure proposed here is composed of a laminated substrate of graphite/epoxy composite coupled with distributed sensor and actuator layers of a biaxially polarized piezoelectric polymer, polyvinylidene fluoride (PVDF). The study aims at investigating the capability of the actuator and sensor layers to cause and sense the deformations, respectively, of the substrate of the intelligent structure. The results show that the effectiveness of the piezoelectric actuator layer to cause induced strain actuation in the structure significantly increases with the decrease in the length to thickness ratio of the substrate.

Introduction

An intelligent structure is made up of a purely elastic material, called the substrate, integrated with distributed actuators and/or sensors. This structure is capable of achieving shape control as soon as it is deformed. A recent trend shows the effectiveness of piezoelectric materials as both distributed sensors and actuators. These materials induce an electric potential/charge when they are subjected to a mechanical deformation by virtue of the direct piezoelectric effect and are deformed due to the externally applied voltage/charge by virtue of the converse piezoelectric effect.

So far several papers have been devoted to the study of intelligent structures. These include analytical treatment with some assumptions or approximate techniques. Broadly, in all of these papers, the attention is focused on the study of the nature of the distributed sensing of deformations and induced strain actuation of the load bearing structures, such as plates and beams. A good account of these papers may be found in a recent paper by Ray et al.[1] and in the technical reports by Ray et al.[2,3] Exact solution for static analysis of intelligent structures under cylindrical bending is presented in a recent work.[2] However, the exact solution for the analysis of intelligent structures under more general deformations is not available. Ray et al.[3] obtained the exact solution for static electroelastic behavior of a piezoelectric material, polyvinylidene fluoride (PVDF). The three-dimensional effects of the applied voltage in this material can be used as a guideline to study the performance of this material when coupled with a substrate (i.e., the load bearing structure) to form an intelligent structure.

In this paper the authors present the exact analysis of simply supported rectangular plate-type intelligent structures without making any assumption about how the piezoelectric sensor and actuator layers are deformed. The intelligent structure proposed here is treated as a laminated plate, and the distributed piezoelectric sensor and actuator layers are considered to be the plies of the laminated intelligent structure and to be bonded perfectly to the surface of the substrate. The substrate is a laminate of graphite/epoxy composite. The interactions of the sensor and actuator layers with the substrate are considered in the same manner as the interactions between two laminae of the substrate. The present analysis will be helpful for further analyses of intelligent structures of complicated geometry and other boundary conditions using improved approximate techniques.

Received Aug. 22, 1992; revision received Jan. 5, 1993; accepted for publication Feb. 4, 1993.

*Research Scholar, Mechanical Engineering Department.
†Assistant Professor, Mechanical Engineering Department.

Procedure for Solutions

Figure 1 shows a simply supported rectangular intelligent structure on the xz plane. The length and breadth of the plate are denoted by a and b, respectively. The top and bottom layers serve as the distributed actuator and sensor, respectively. The material of the distributed sensor and actuator is the so-called piezoelectric polymer PVDF. The substrate is a laminate of any number of layers of orthotropic materials. The axes of elastic symmetry in the orthotropic layers are parallel to the reference axes. The exact analysis of a laminated-type intelligent structure requires determination of the stresses, strains, and displacements at any point in any layer of the structure satisfying all of the governing field equations, stress-strain relations, and strain-displacement relations for that layer subjected to known boundary conditions and interface continuity conditions. The closed-form expressions for the stresses and displacements for an orthotropic layer under simply supported boundary conditions are available[4] and will be directly used to show the performance of the distributed piezoelectric sensor and actuator. Hence, only the expressions for the stresses and displacements in the piezoelectric sensor and actuator layers are derived and presented in the following.

The linear constitutive equations coupling the elastic and electric fields in a piezoelectric medium are given by[5]

$$\{D\} = [e]^T\{\epsilon\} + [\epsilon]\{E\}$$

$$\{\sigma\} = [C]\{\epsilon\} - [e]\{E\} \tag{1a}$$

where $\{D\}$, $\{E\}$, $\{\epsilon\}$, and $\{\sigma\}$ are the electric displacement, electric field, strain, and stress vectors, respectively, and $[C]$, $[e]$, and $[\epsilon]$ are the elasticity, piezoelectric, and dielectric constant matrices, respectively, with $[e]^T$ defined as the transpose of $[e]$.

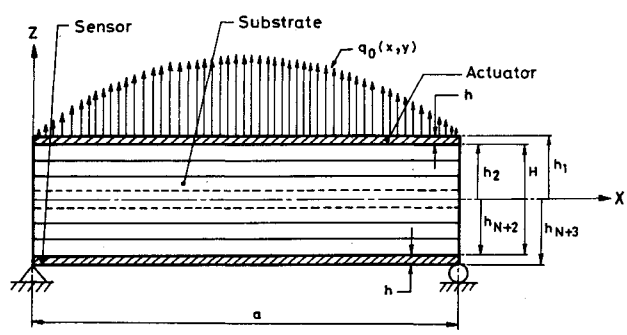

Fig. 1 Plate configuration.

The piezoelectric constant matrix $[e]^T$ and the dielectric matrix $[\epsilon]$ for the PVDF polymer are given by Cady,[6] and Tzou and Pandita[7] as

$$[e]^T = \begin{bmatrix} 0 & 0 & 0 & 0 & e_{15} & 0 \\ 0 & 0 & 0 & e_{24} & 0 & 0 \\ e_{31} & e_{32} & e_{33} & 0 & 0 & 0 \end{bmatrix}$$

$$[\epsilon] = \begin{bmatrix} \epsilon_{11} & 0 & 0 \\ 0 & \epsilon_{22} & 0 \\ 0 & 0 & e_{33} \end{bmatrix} \tag{1b}$$

The constitutive relations for the piezoelectric layers of the intelligent structure are obtained from Eqs. (1a) and (1b) as

$$\begin{aligned} \sigma_x^k &= C_{11}\epsilon_x^k + C_{12}\epsilon_y^k + C_{13}\epsilon_z^k - e_{31}E_z^k \\ \sigma_y^k &= C_{12}\epsilon_x^k + C_{22}\epsilon_y^k + C_{23}\epsilon_z^k - e_{32}E_z^k \\ \sigma_z^k &= C_{13}\epsilon_x^k + C_{23}\epsilon_y^k + C_{33}\epsilon_z^k - e_{33}E_z^k \\ \sigma_{yz}^k &= C_{44}\epsilon_{yz}^k - e_{24}E_y^k \\ \sigma_{xz}^k &= C_{55}\epsilon_{xz}^k - e_{15}E_x^k \\ \sigma_{xy}^k &= C_{66}\epsilon_{xy}^k \\ D_x^k &= e_{15}\epsilon_{xz}^k + \epsilon_{11}E_x^k \\ D_y^k &= e_{24}\epsilon_{yz}^k + \epsilon_{22}E_y^k \\ D_z^k &= e_{31}\epsilon_x^k + e_{32}\epsilon_y^k + e_{33}\epsilon_z^k + \epsilon_{33}E_z^k \end{aligned} \tag{2}$$

where the superscript k denotes the layer number and for the piezoelectric layers k takes the value 1 and $N+2$, N being the number of layers in the laminated substrate.

The two governing field equations[5] for a piezoelectric medium are given in the following.

The stress equilibrium equations are

$$\begin{aligned} \sigma_{x,x}^k + \sigma_{xy,y}^k + \sigma_{xz,z}^k &= 0 \\ \sigma_{xy,x}^k + \sigma_{y,y}^k + \sigma_{yz,z}^k &= 0 \\ \sigma_{xz,x}^k + \sigma_{yz,y}^k + \sigma_{z,z}^k &= 0 \end{aligned} \tag{3a}$$

The charge equilibrium equation is

$$D_{x,x}^k + D_{y,y}^k + D_{z,z}^k = 0 \tag{3b}$$

where the comma is followed by a quantity representing the partial differentiation with respect to that quantity.

The strain-displacement relations are

$$\begin{aligned} \epsilon_x^k &= \frac{\partial u^k}{\partial x}, \quad \epsilon_y^k = \frac{\partial v^k}{\partial y}, \quad \epsilon_z^k = \frac{\partial w^k}{\partial z} \\ \epsilon_{yz}^k &= \frac{\partial v^k}{\partial z} + \frac{\partial w^k}{\partial y}, \quad \epsilon_{xz}^k = \frac{\partial u^k}{\partial z} + \frac{\partial w^k}{\partial x} \\ \epsilon_{xy}^k &= \frac{\partial u^k}{\partial y} + \frac{\partial v^k}{\partial x} \end{aligned} \tag{3c}$$

and the electric field-potential relations are given by

$$E_x^k = -\frac{\partial \phi^k}{\partial x}, \quad E_y^k = -\frac{\partial \phi^k}{\partial y}, \quad E_z^k = -\frac{\partial \phi^k}{\partial z} \tag{3d}$$

where u^k, v^k, and w^k are the mechanical displacement components along the x, y, and z axes, respectively, in the kth layer, and ϕ^k is the electric potential function.

Use of Eqs. (3c) and (3d) in Eqs. (3a) and (3b) yields

$$C_{11}u^k_{,xx} + (C_{12} + C_{66})v^k_{,xy} + (C_{13} + C_{55})w^k_{,xz} + C_{66}u^k_{,yy} + C_{55}u^k_{,zz} + (e_{31} + e_{15})\phi^k_{,xz} = 0 \tag{4}$$

$$(C_{12} + C_{66})u^k_{,xy} + C_{66}v^k_{,xx} + C_{22}v^k_{,yy} + (C_{23} + C_{44})w^k_{,yz} + C_{44}v^k_{,zz} + (e_{32} + e_{24})\phi^k_{,yz} = 0 \tag{5}$$

$$(C_{13} + C_{55})u^k_{,xz} + (C_{23} + C_{44})v^k_{,yz} + C_{55}w^k_{,xx} + C_{33}w^k_{,zz} + e_{15}\phi^k_{,xx} + e_{24}\phi^k_{,yy} + e_{33}\phi^k_{,zz} = 0 \tag{6}$$

$$(e_{15} + e_{31})u^k_{,xz} + e_{15}w^k_{,xx} + (e_{24} + e_{32})v^k_{,yz} + e_{24}w^k_{,yy} + e_{33}w^k_{,zz} - \epsilon_{11}\phi^k_{,xx} - \epsilon_{22}\phi^k_{,yy} - \epsilon_{33}\phi^k_{,zz} = 0 \tag{7}$$

The solutions of Eqs. (4–7) are sought for SS3 boundary conditions,[8] which translate into

$$\begin{aligned} \sigma_x^k = v^k = w^k = 0 \\ \sigma_y^k = u^k = w^k = 0 \\ x = 0 \text{ and } a, \text{ and } y = 0 \text{ and } b \end{aligned} \tag{8a}$$

Also, the edges are suitably grounded so that the electric potential at the edges are zero,[1] i.e., that

$$\phi^k = 0 \text{ at } x = 0, a \text{ and } y = 0, b \tag{8b}$$

The displacement functions and the electric potential function that exactly satisfy the boundary conditions (8a) and (8b), respectively, have the form

$$\begin{aligned} u^k &= U^k(z)\cos px \sin qy \\ v^k &= V^k(z)\sin px \cos qy \\ w^k &= W^k(z)\sin px \sin qy \\ \phi^k &= \Phi^k(z)\sin px \sin qy \end{aligned} \tag{9}$$

where $p = m\pi/a$, $q = n\pi/b$, and m and n are nonzero integers. The results obtained here may be modified easily in the more general case where Eq. (9) has a double Fourier series representation with more than one combination of integers m and n.

Following Pagano,[4] let us assume that

$$(U^k, V^k, W^k, \Phi^k) = (U^{0k}, V^{0k}, W^{0k}, \Phi^{0k})e^{tz} \tag{10}$$

where U^{0k}, V^{0k}, W^{0k}, Φ^{0k}, and t are unknown constants. Then, substitution of Eqs. (9) and (10) in Eqs. (4–7) yields the following set of homogeneous algebraic equations in terms of the unknowns U^{0k}, V^{0k}, W^{0k}, and Φ^{0k}:

$$(C_{55}t^2 - C_{11}p^2 - C_{66}q^2)U^{0k} - pq(C_{12} + C_{66})V^{0k} + pt(C_{13} + C_{55})W^{0k} + pt(e_{31} + e_{15})\Phi^{0k} = 0 \tag{11}$$

$$-pq(C_{66} + C_{12})U^{0k} + (C_{44}t^2 - C_{66}p^2 - C_{22}q^2)V^{0k} + qt(C_{23} + C_{44})W^{0k} + qt(e_{32} + e_{24})\Phi^{0k} = 0 \tag{12}$$

$$-pt(C_{13} + C_{55})U^{0k} - qt(C_{23} + C_{44})V^{0k} + (C_{33}t^2 - C_{55}p^2 - C_{44}q^2)W^{0k} + (e_{33}t^2 - e_{15}p^2 - e_{24}q^2)\Phi^{0k} = 0 \tag{13}$$

$$-pt(e_{15} + e_{31})U^{0k} - qt(e_{24} + e_{32})V^{0k} + (e_{33}t^2 - e_{15}p^2 - e_{24}q^2)W^{0k} + (\epsilon_{11}p^2 + \epsilon_{22}q^2 - \epsilon_{33}t^2)\Phi^{0k} = 0 \tag{14}$$

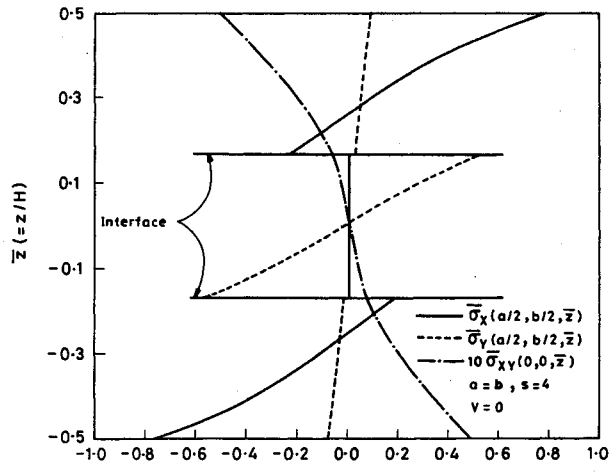

Fig. 2 Distribution of in-plane stresses across the thickness without prescribed electric potential on the surface of the actuator.

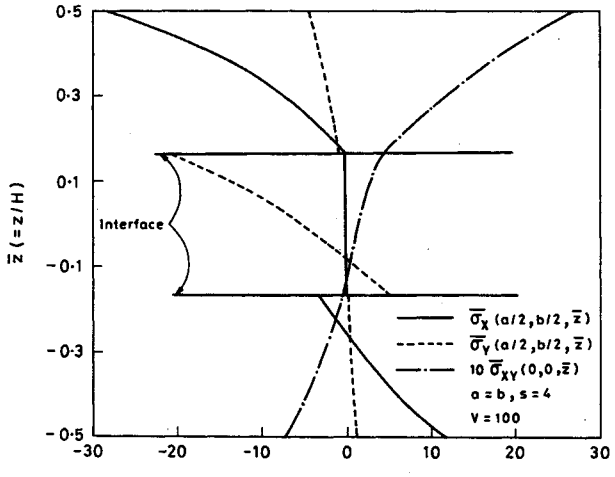

Fig. 3 Distribution of in-plane stresses across the thickness with prescribed electric potential on the surface of the actuator.

The piezoelectric material considered here is elastically isotropic and biaxially polarized. A voltage or electric field applied across the faces (perpendicular to the z axis) of the plate results in longitudinal strains in both x and y directions owing to the piezoelectric constants e_{31} and e_{32}. The other constants e_{15}, e_{24}, and e_{33} are considered to be absent in the medium.[9] Since $e_{31} = e_{32}$ and also $\epsilon_{11} = \epsilon_{22} = \epsilon_{33}$ (Tzou and Tseng[9]), the relation between U^{0k} and V^{0k} may be obtained from Eqs. (11) and (12) as

$$V^{0k} = \frac{q}{p} U^{0k} \tag{15}$$

Equation (15) is now used in Eqs. (13) and (14) to obtain W^{0k} and Φ^{0k} in terms of U^{0k} as follows:

$$W^{0k} = \frac{t(C_{12} + C_{44})(p^2 + q^2)}{p[C_{11}t^2 - C_{44}(p^2 + q^2)]} U^{0k} \tag{16}$$

$$\Phi^{0k} = \frac{te_{31}(p^2 + q^2)}{p\epsilon_{11}(p^2 + q^2 - t^2)} U^{0k} \tag{17}$$

Finally, to find the nontrivial solution of U^{0k}, Eqs. (15–17) are used in Eqs. (11) and the following polynomial equation is obtained:

$$At^6 + Bt^4 + Ct^2 + D = 0 \tag{18}$$

where for the material considered the coefficients A, B, C, and D are simplified as

$$A = -C_{11}C_{44}\epsilon_{11}, \qquad B = C_{11}(3C_{44}\epsilon_{11} + e_{31}^2)(p^2 + q^2)$$

$$C = -(3C_{44}C_{11}\epsilon_{11} + C_{44}e_{31}^2)(p^2 + q^2)^2$$

$$D = \epsilon_{11}C_{11}C_{44}(p^2 + q^2)^3 \tag{18a}$$

Thus, from Eqs. (18) and (18a) and the definitions of p and q given after Eq. (9), it follows that the value of t depends on the elastic, dielectric, and piezoelectric constants as well as on the geometry and the integers m and n.

Equation (18) can be transformed into the standard cubic equation as

$$\zeta^3 + g\zeta + f = 0 \tag{19a}$$

with

$$\zeta = t^2 + \frac{B}{3A}$$

$$g = -\frac{B^2 - 3AC}{3A^2}, \qquad f = \frac{2B^3 - 9ABC + 27A^2D}{27A^3} \tag{19b}$$

The solutions of Eq. (19a) depend on the sign of the quantity Q given by

$$Q = \frac{f^2}{4} + \frac{g^3}{27}$$

Here Q is positive for the material considered, and the solutions of Eq. (19a) can be obtained as

$$(\gamma + \delta), \quad \left[-\frac{1}{2}(\gamma + \delta) + i\frac{\sqrt{3}}{2}(\gamma - \delta)\right], \quad \left[-\frac{1}{2}(\gamma + \delta) - i\frac{\sqrt{3}}{2}(\gamma - \delta)\right] \tag{20}$$

where

$$\gamma = \{\tfrac{1}{2}(-f + 2\sqrt{Q})\}^{1/3}, \qquad \delta = \{\tfrac{1}{2}(-f - 2\sqrt{Q})\}^{1/3}$$

Substitution of Eq. (20) into Eq. (19b) yields the following six roots of Eq. (18).

First pair: either $\pm\lambda$ $\left(\text{if } \gamma + \delta - \frac{B}{3A} > 0\right)$

or $\pm i\lambda$ $\left(\text{if } \gamma + \delta - \frac{B}{3A} < 0\right)$

Second pair: $\pm(\alpha + i\beta)$

Third pair: $\pm(\alpha - i\beta)$

where

$$\lambda = \left\{\left|\gamma + \delta - \frac{B}{3A}\right|\right\}^{1/2}$$

$$\alpha = (a_1^2 + b_1^2)^{1/4} \cos\left(\frac{1}{2}\tan^{-1}\frac{b_1}{a_1}\right)$$

$$\beta = (a_1^2 + b_1^2)^{1/4} \sin\left(\frac{1}{2}\tan^{-1}\frac{b_1}{a_1}\right)$$

$$a_1 = \tfrac{1}{2}(\gamma + \delta) - \frac{B}{3A} \qquad b_1 = \frac{\sqrt{3}}{2}(\gamma - \delta)$$

In the present case, the first pair of roots are real. Use of these roots along with Eqs. (9), (10), and (15–17) leads to the

general solutions of u^k, v^k, w^k, and ϕ^k as follows:

$$u^k = [(F_{1k}\cosh \lambda z + G_{1k}\sinh \lambda z) + e^{\alpha z}(F_{2k}\cos \beta z + G_{2k}\sin \beta z) + e^{\alpha z}(F_{3k}\cos \beta z - G_{3k}\sin \beta z)]\cos px \sin qy$$

$$v^k = (q/p)[F_{1k}\cosh \lambda z + G_{1k}\sinh \lambda z) + e^{\alpha z}(F_{2k}\cos \beta z + G_{2k}\sin \beta z) + e^{-\alpha z}(F_{3k}\cos \beta z - G_{3k}\sin \beta z)]\sin px \cos qy$$

$$w^k = [Q_1(F_{1k}\sinh \lambda z + G_{1k}\cosh \lambda z) + Q_2 e^{\alpha z}(F_{2k}\cos \beta z + G_{2k}\sin \beta z) - Q_2 e^{-\alpha z}(F_{3k}\cos \beta z - G_{3k}\sin \beta z) + Q_3 e^{\alpha z}(G_{2k}\cos \beta z - F_{2k}\sin \beta z) - Q_3 e^{-\alpha z}(G_{3k}\cos \beta z + F_{3k}\sin \beta z)]\sin px \sin qy$$

$$\phi^k = [R_1(F_{1k}\sinh \lambda z + G_{1k}\cosh \lambda z) + R_2 e^{\alpha z}(F_{2k}\cos \beta z + G_{2k}\sin \beta z) - R_2 e^{-\alpha z}(F_{3k}\cos \beta z - G_{3k}\sin \beta z) + R_3 e^{\alpha z}(G_{2k}\cos \beta z - F_{2k}\sin \beta z) - R_3 e^{-\alpha z}(G_{3k}\cos \beta z + F_{3k}\sin \beta z)]\sin px \sin qy \quad (21)$$

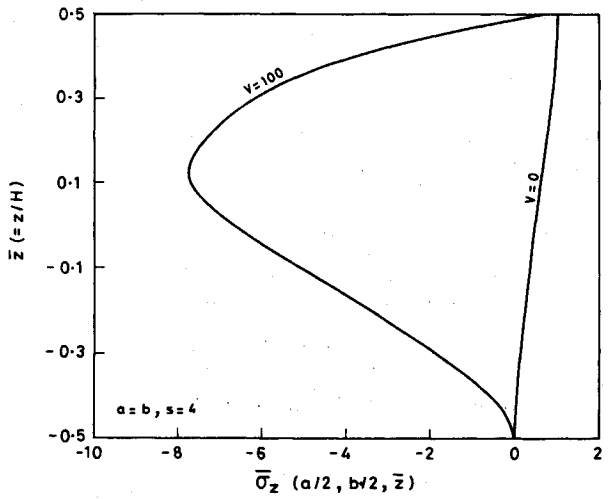

Fig. 4 Distribution of transverse normal stress across the thickness.

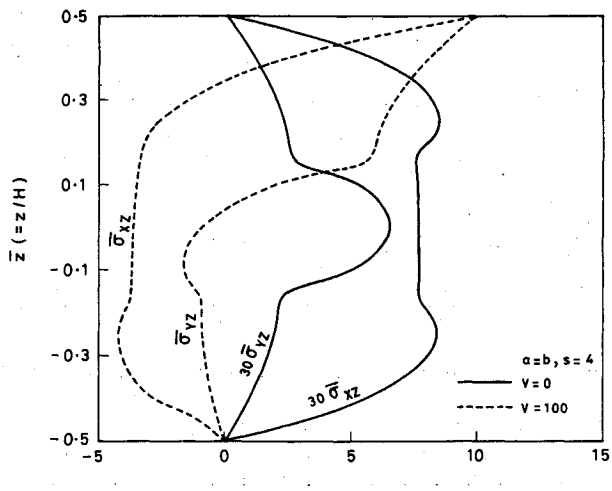

Fig. 5 Distribution of transverse shear stresses across the thickness.

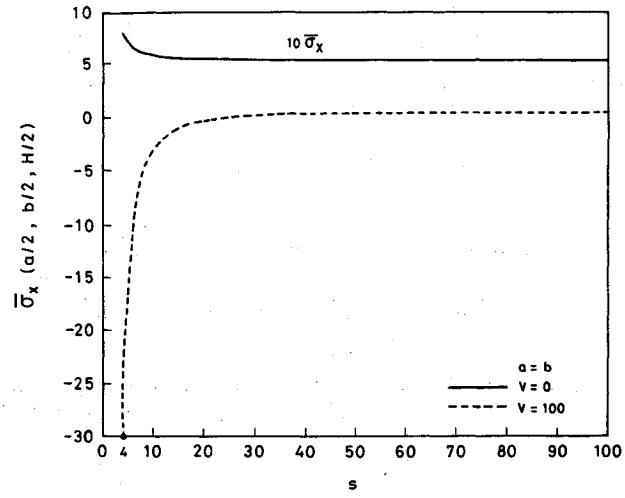

Fig. 6 Maximum in-plane normal stress ($\bar{\sigma}_x$) for various span to thickness ratios.

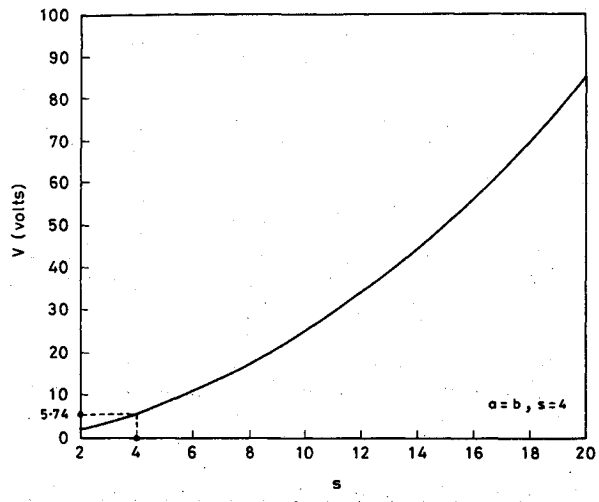

Fig. 7 Values of V to make the midplane deflection zero for various span to thickness ratios.

where F_{jk}, and G_{jk} (j = 1, 2, 3) are unknown constants to be evaluated from boundary conditions. Note that the subscript k also takes the value for the layer number of piezoelectric layers. Various other quantities appearing in Eqs. (21) are defined as follows.

$$Q_1 = \frac{\lambda(p^2+q^2)(C_{12}+C_{44})}{p[C_{11}\lambda^2 - C_{44}(p^2+q^2)]}$$

$$Q_2 = \frac{(p^2+q^2)(C_{12}+C_{44})(\alpha c_1 + \beta d_1)}{p(c_1^2+d_1^2)}$$

$$Q_3 = \frac{(p^2+q^2)(C_{12}+C_{44})(\beta c_1 - \alpha d_1)}{p(c_1^2+d_1^2)}$$

$$c_1 = c_{11}a_1 - c_{44}(p^2+q^2) \qquad c_2 = p^2+q^2-a_1$$

$$R_1 = \frac{\lambda e_{31}(p^2+q^2)}{\epsilon_{11}p(p^2+q^2-\lambda^2)}$$

$$R_2 = \frac{e_{31}(p^2+q^2)(\alpha c_2 + \beta d_2)}{\epsilon_{11}p(c_2^2+d_2^2)}$$

$$R_3 = \frac{e_{31}(p^2+q^2)(\beta c_2 - \alpha d_2)}{\epsilon_{11} p (c_2^2 + d_2^2)}$$

$$d_1 = c_{11} b_1 \qquad d_2 = -b_1$$

Finally, using the strain-displacement relations in conjunction with Eqs. (1a) and (21), the following expressions for stresses and electric displacement are obtained:

$$\sigma_x^k = [(F_{1k}\cosh \lambda z + G_{1k}\sinh \lambda z)T_1 + F_{2k}(T_2 \cos \beta z - T_3 \sin \beta z)e^{\alpha z} + G_{2k}(T_3 \cos \beta z + T_2 \sin \beta z)e^{\alpha z} + F_{3k}(T_2 \cos \beta z + T_3 \sin \beta z)e^{-\alpha z} + G_{3k}(T_3 \cos \beta z - T_2 \sin \beta z)e^{-\alpha z}] \sin px \sin qy$$

$$\sigma_y^k = [(F_{1k}\cosh \lambda z + G_{1k}\sinh \lambda z)T_4 + F_{2k}(T_5 \cos \beta z - T_6 \sin \beta z)e^{\alpha z} + G_{2k}(T_6 \cos \beta z + T_5 \sin \beta z)e^{\alpha z} + F_{3k}(T_5 \cos \beta z + T_5 \sin \beta z)e^{-\alpha z} + G_{3k}(T_6 \cos \beta z - T_5 \sin \beta z)e^{-\alpha z}] \sin px \sin qy$$

$$\sigma_z^k = [(F_{1k}\cosh \lambda z + G_{1k}\sinh \lambda z)T_7 + F_{2k}(T_8 \cos \beta z - T_9 \sin \beta z)e^{\alpha z} + G_{2k}(T_9 \cos \beta z + T_8 \sin \beta z)e^{\alpha z} + F_{3k}(T_8 \cos \beta z + T_9 \sin \beta z)e^{-\alpha z} + G_{3k}(T_9 \cos \beta z - T_8 \sin \beta z)e^{-\alpha z}] \sin px \sin qy$$

$$\sigma_{xz}^k = [(F_{1k}\sinh \lambda z + G_{1k}\cosh \lambda z)T_{10} + F_{2k}(T_{11} \cos \beta z - T_{12} \sin \beta z)e^{\alpha z} + G_{2k}(T_{12} \cos \beta z + T_{11} \sin \beta z)e^{\alpha z} + F_{3k}(T_{11} \cos \beta z + T_{12} \sin \beta z)e^{-\alpha z} + G_{3k}(T_{12} \cos \beta z - T_{11} \sin \beta z)e^{-\alpha z}] \cos px \sin qy$$

$$\sigma_{yz}^k = (q/p)[(F_{1k}\sinh \lambda z + G_{1k}\cosh \lambda z)T_{10} + F_{2k}(T_{11} \cos \beta z - T_{12} \sin \beta z)e^{\alpha z} + G_{2k}(T_{12} \cos \beta z + T_{11} \sin \beta z)e^{\alpha z} + F_{3k}(T_{11} \cos \beta z + T_{12} \sin \beta z)e^{-\alpha z} + G_{3k}(T_{12} \cos \beta z - T_{11} \sin \beta z)e^{-\alpha z}] \cos px \sin qy$$

$$\sigma_{xy}^k = 2qC_{44}[F_{1k}\cosh \lambda z + G_{1k}\sinh \lambda z + e^{\alpha z}(F_{2k}\cos \beta z + G_{2k}\sin \beta z + e^{-\alpha z}F_{3k}\cos \beta z - G_{3k}\sin \beta z)] \cos px \cos qy$$

$$D_z^k = [(F_{1k}\sinh \lambda z + G_{1k}\cosh \lambda z)T_{13} + F_{2k}(T_{14} \cos \beta z + T_{15} \sin \beta_z)e^{\alpha z} - G_{2k}(T_{15}\cos \beta z - T_{14} \sin \beta z)e^{\alpha z} + F_{3k}(T_{14} \cos \beta z - T_{15} \sin \beta z)e^{-\alpha z} - G_{3k}(T_{15} \cos \beta z + T_{14} \sin \beta z)e^{-\alpha z}] \sin px \sin qy \qquad (22)$$

where

$$T_1 = -pC_{11} - (q^2/p)C_{12} + \lambda Q_1 C_{13} + \lambda R_1 e_{31}$$

$$T_2 = -pC_{11} - (q^2/p)C_{12} + C_{13}(\alpha Q_2 - \beta Q_3) + e_{31}(\alpha R_2 - \beta R_3)$$

$$T_3 = C_{13}(\alpha Q_3 + \beta Q_2) + e_{31}(\alpha R_3 + \beta R_2)$$

$$T_4 = -pC_{12} - (q^2/p)C_{22} + \lambda Q_1 C_{23} + \lambda R_1 e_{32}$$

$$T_5 = -pC_{12} - (q^2/p)C_{22} + C_{23}(\alpha Q_2 - \beta Q_3) + e_{32}(\alpha R_2 - \beta R_3)$$

$$T_6 = C_{23}(\alpha Q_3 - \beta Q_2) + e_{32}(\alpha R_3 - \beta R_2)$$

$$T_7 = -pC_{13} - (q^2/p)\,C_{23} + \lambda Q_1 C_{33}$$

$$T_8 = -pC_{13} - (q^2/p)C_{23} + C_{33}(\alpha Q_2 - \beta Q_3)$$

$$T_9 = C_{33}(\alpha Q_3 + \beta Q_2) \qquad T_{10} = C_{44}(\lambda + pQ_1)$$

$$T_{11} = C_{44}(\alpha + pQ_2) \qquad T_{12} = C_{44}(\beta + pQ_3)$$

$$T_{13} = -pe_{31} - (q^2/p)e_{31} - \epsilon_{33}\lambda R_1$$

$$T_{14} = -pe_{31} - (q^2/p)e_{31} - \epsilon_{33}(\alpha R_2 - \beta R_3)$$

$$T_{15} = \epsilon_{33}(\alpha R_3 + \beta R_2)$$

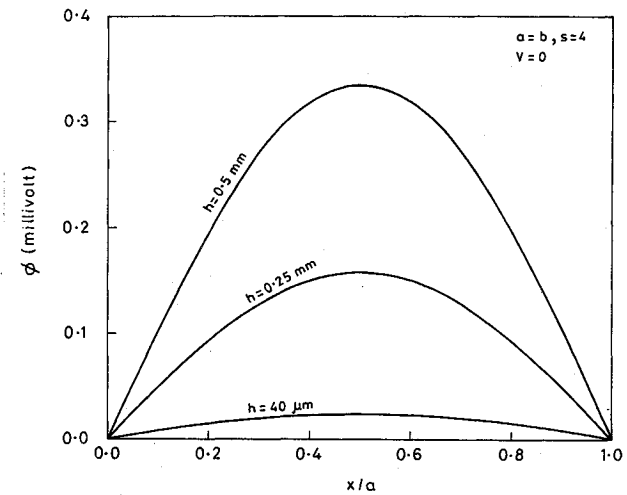

Fig. 8 Distribution of induced electric potential on the surface of the sensor along the length ($y = b/2$) of the plate without prescribed electric potential on the surface of the actuator.

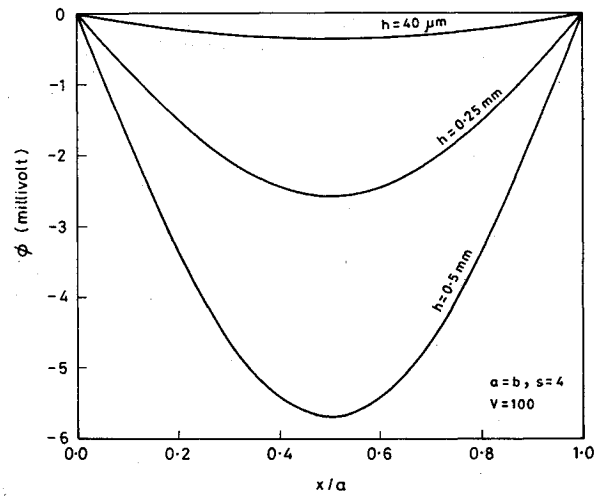

Fig. 9 Distribution of induced electric potential on the surface of the sensor along the length ($y = b/2$) of the plate with prescribed electric potential on the surface of the actuator.

The expressions for D_x^k and D_y^k are not given here and can be obtained from the constitutive equations. As a check, the derived expressions for stresses and electric displacements are found to satisfy the governing Eqs. (3a) and (3b).

In what follows, the boundary conditions for the top and bottom surfaces are discussed. Since the surfaces of the overall structure are made of the piezoelectric material, both the electrical and mechanical boundary conditions are to be prescribed to evaluate the system behavior. In a piezoelectric continuum, one may specify the electric potential or the free charge density[5,10] over the portions of the boundary. The relation between the free charge density $\bar{\sigma}$ and the electric displacement vector $D_r (r = x, y, z)$ on the surface of a piezoelectric continuum is given by[5]

$$\bar{\sigma} + n_r D_r = 0 \tag{23}$$

Here n_r are the direction cosines of the unit normal to the surface considered for the specification of free charge density. Thus if we specify zero free charge density on the surface normal to the z axis, then Eq. (23) yields zero value of D_z on that surface. This can be used as the boundary condition for that surface. Therefore, the specification of boundary conditions will determine the behavior of the piezoelectric layers acting as a sensor and an actuator. Accordingly, the boundary conditions for the overall structure can be taken as follows:

1) On the surface of the piezoelectric layer that behaves as an actuator

$$\sigma_z^1(x,y,h_1) = q_0(x,y) \qquad \sigma_{xz}^1(x,y,h_1) = 0$$

$$\sigma_{yz}^1(x,y,h_1) = 0 \qquad \phi^1(x,y,h_1) = \Phi_1(x,y) \tag{24}$$

where $q_0(x,y)$ and $\Phi_1(x,y)$ are the prescribed surface traction and the electric potential distribution function, respectively.

2) On the surface of the piezoelectric layer that acts as a sensor

$$\sigma_z^{N+2}(x,y,h_{N+3}) = 0 \qquad \sigma_{xz}^{N+2}(x,y,h_{N+3}) = 0$$

$$\sigma_{yz}^{N+2}(x,y,h_{N+3}) = 0 \qquad D_z^{N+2}(x,y,h_{N+3}) = 0 \tag{25}$$

Also the following interface conditions must be satisfied:

$$\Phi^1(x,y,h_2) = 0 \qquad \Phi^{N+2}(x,y,h_{N+2}) = 0$$

$$u^k(x,y,h_{k+1}) = u^{k+1}(x,y,h_{k+1})$$

$$v^k(x,y,h_{k+1}) = v^{k+1}(x,y,h_{k+1})$$

$$w^k(x,y,h_{k+1}) = w^{k+1}(x,y,h_{k+1})$$

$$\sigma_z^k(x,y,h_{k+1}) = \sigma_z^{k+1}(x,y,h_{k+1})$$

$$\sigma_{xz}^k(x,y,h_{k+1}) = \sigma_{xz}^{k+1}(x,y,h_{k+1})$$

$$\sigma_{yz}^k(x,y,h_{k+1}) = \sigma_{yz}^{k+1}(x,y,h_{k+1}) \tag{26}$$

wherein $k = 1, 2, 3, \ldots, N+1$.

The expressions of stresses and displacements for an orthotropic layer of a laminated plate obtained by Pagano[4] contain six unknown constants. Also, the derived expressions for the stresses, displacements, and electric potential functions for each piezoelectric layer contain six unknowns. Thus, the analysis of the overall structure requires solution of $6(N+2)$ unknown constants. But the solutions need to satisfy eight boundary conditions given by Eqs. (24) and (25) and $(6N+8)$ interface conditions given by Eqs. (26). Hence, the total number of conditions to be satisfied turns out to be greater than the number of unknowns to be found. To introduce four additional unknown constants, the expressions for v^k, and $\sigma_{yz}^k (k = 1$ and $N+2)$, given by Eqs. (21) and (22), respectively, are modified. Note that in performing this modification the governing field equations are still satisfied. The results are

$$\begin{aligned} v^k = \{ & F \cosh \lambda z + G_{4k} \sinh \lambda z + (q/p)[e^{\alpha z}(F_{2k} \cos \beta z \\ & + G \sin \beta z) + e^{-\alpha z}(F_{3k} \cos \beta z \\ & - G_{4k} \sin \beta z)]\} \sin px \cos qy \end{aligned}$$

$$\begin{aligned} \sigma_{yz}^k = \{ & (F_{4k} \sinh \lambda z + G_{4k} \cosh \lambda z) T_{10} \\ & + (q/p)[F_{2k}(T_{11} \cos \beta z - T_{12} \sin \beta z) e^{\alpha z} \\ & + G_{2k}(T_{12} \cos \beta z + T_{11} \sin \beta z) e^{\alpha z} + F_{3k}(T_{11} \cos \beta z \\ & + T_{12} \sin \beta z) e^{-\alpha z} + G_{3k}(T_{12} \cos \beta z \\ & - T_{11} \sin \beta z) e^{-\alpha z}]\} \sin px \cos qy \end{aligned} \tag{27}$$

Here, the additional unknown constants F_{4k} and G_{4k} are introduced as follows:

$$F_{4k} = (q/p) F_{1k} \qquad G_{4k} = (q/p) G_{1k}$$

With these modifications the system is now sufficient to solve for the unknowns satisfying all the boundary and interface conditions. Imposing the boundary and interface conditions given by Eqs. (24–26) one can obtain the system response with $q_0(x,y) = \sigma \sin px \sin qy$, and $\Phi(x,y) = V \sin px \sin qy$, where $\sigma (\mathrm{N/m^2})$ and V (volt) are constants. Note that once the unknowns are evaluated, one can use either the modified expressions for v^k and σ_{yz}^k as given by Eqs. (27) or the expressions derived earlier in Eqs. (21) and (22) to obtain the layer-wise system response.

Results

Specific results are presented for the intelligent plate, the substrate of which is a three-layered (0/90/0 deg) bidirectional laminate made of graphite/epoxy composite.

Using the material properties for the piezoelectric layer from Tzou and Tseng[9] and those for the orthotropic layers in the substrate from Pagano,[4] and considering $m = n = 1$ in the definition of p and q, the unknowns and the numerical results are evaluated with distributed sinusoidal mechanical load and with or without creating the electric potential distribution on the actuator surface for different values of length to thickness ratio, s ($= a/H$, with H the thickness of the substrate).

Table 1 Comparison of substrate response for negligible h and $V = 0$ with that of an identical laminate obtained by Pagano[4]

Source	s	b/a	u*	w*	σ_x^*	σ_y^*	σ_{xz}^*	σ_{yz}^*	σ_{xy}^{*a}
Present analysis	4	1	−.0097 .0094	1.99	.801 −.756	.534 −.559	.256	.2170	−.0511 .0502
Pagano[4]	4	1	−.0097 .0094	1.99	.801 −.756	.534 −.556	.256	.2172	−.0511 .0505
Present analysis	100	1	±.0067	.47	±.539	±.181	.395	.0828	∓.0214
Pagano[4]	100	1	±.0067	.47	±.539	±.181	.395	.0828	∓.0213
Present analysis	4	3	−.0143 .0141	2.82	1.14 −1.10	.105 −.12	.351	.033	−.0268 .0264
Pagano[4]	4	3	−.0142 .0139	2.82	1.14 −1.10	.109 −.119	.351	.0334	−.0269 .0261

[a] $\sigma_x^* = \bar{\sigma}_x(a/2, b/2, \pm H/2)$, $\sigma_y^* = \bar{\sigma}_y(a/2, b/2, \pm H/6)$, $\sigma_{xz}^* = \bar{\sigma}_{xz}(0, b/2, 0)$, $\sigma_{yz}^* = \bar{\sigma}_{yz}(a/2, 0, 0)$, $\sigma_{xy}^* = \bar{\sigma}_{xy}(0, 0, \pm H/2)$, $u^* = \bar{u}(0, b/2, \pm H/2)$, $w^* = \bar{w}(a/2, b/2, 0)$.

Table 2 Response in the substrate of the square intelligent structure

s	V	σ_x^*	σ_y^*	σ_z^{*a}	σ_{xz}^*	σ_{yz}^*	σ_{xy}^*	u^*	w^*
4	0	.799 −.754	.532 −.557	.492	.256	.217	−.051 .049	−.0097 .0094	1.99
	100	−29.29 11.78	−21.24 5.21	−6.68	−3.625	−.910	2.706 −.728	.358 −.146	−31.56
6	0	.668 −.659	.406 −.418	.497	.31	.169	−.038 .038	∓.0082	1.24
	100	−10.83 5.09	−8.155 .9452	−3.09	−2.033	.210	.80 −.263	.134 −.064	−10.17
10	0	±.589	.284 −.288	.499	.357	.123	−.0287 .0288	∓.0073	.774
	100	−3.12 1.48	−2.34 −.261	−.878	−.683	.336	.181 −.058	.0388 −.0186	−2.35
20	0	.552 −.552	.209 −.209	.499	.384	.094	−.023 .023	∓.0069	.549
	100	−3.21 −.039	−.372 −.277	.145	.145	.096	.017 .005	.004 .0005	−.095
100	0	.538 −.538	.181 −.181	.50	.394	.083	−.021 .021	∓.0067	.471
	100	−.504 −.518	.158 −.184	.486	.382	.086	−.019 .021	−.0063 .0065	.447

[a] $\sigma_z^* = \bar{\sigma}_z(a/2, b/2, 0)$.

The results are nondimensionalized as

$$(\bar{\sigma}_x, \bar{\sigma}_y, \bar{\sigma}_{xy}) = \frac{1}{\sigma s^2}(\sigma_x^k, \sigma_y^k, \sigma_{xy}^k)$$

$$(\bar{\sigma}_{xz}, \bar{\sigma}_{yz}) = \frac{1}{\sigma s}(\sigma_{xz}^k, \sigma_{yz}^k) \qquad \bar{\sigma}_z = \frac{1}{\sigma}\sigma_z^k$$

$$\bar{u} = \frac{E_T}{\sigma s^3 H} u \qquad \bar{w} = \frac{100 E_T}{\sigma s^4 H} w$$

where E_T is the transverse Young's modulus of the orthotropic layers.

If the thickness and weight of the piezoelectric sensor and actuator layers are very much less than those of the substrate, the static and dynamic behaviors of the substrate of an intelligent structure without the applied voltage to the actuator do not differ significantly from those of a structure identical to the substrate under the same mechanical boundary conditions.[11] Hence, to check the numerical results, the mechanical displacements and stresses in the laminated substrate of the intelligent structure obtained without applied voltage to the actuator are compared to those obtained by Pagano[4] for a laminate identical to the present substrate for various values of s. The results are found to match very well (see Table 1) when the thickness of the sensor and actuator layers are negligibly small in comparison to the thickness of the substrate, say 0.0011% of that substrate. Next, taking the value of the thickness of the sensor and actuator layers as 40μm[9] and using the value for the thickness of each layer of the substrate as 3 mm, the response of the substrate of the proposed intelligent structure has been computed. These results are shown in Figs. 2–9 for $s = 4$ and in Table 2 for several values of s. Figures 2 and 3 illustrate the distribution of inplane stresses ($\bar{\sigma}_x$, $\bar{\sigma}_y$, and $\bar{\sigma}_{xy}$) in the layers of the laminated substrate without and with the electric potential distribution on the actuator surface. It is evident from these figures that the actuator counteracts the mechanical loading. For example, the distribution of $\bar{\sigma}_x$ implies that the top and bottom layers of the substrate undergo bending mainly when $V = 0$ (Fig. 2). Due to the combined action of actuator and mechanical loading, these layers also undergo bending predominantly but in a reverse way when $V = 100$ (Fig. 3). The maximum value of $\bar{\sigma}_x$ is more than 35 times of that at $V = 0$. Since the fiber direction of the middle layer of the substrate is along the y axis, the distribution of $\bar{\sigma}_y$ in the middle layer is significantly affected (Figs. 2 and 3). Figures 2 and 3 also show that the actuator causes a significant effect on the inplane shear in the layers of the substrate caused by the mechanical loading alone. The maximum value of $\bar{\sigma}_{xy}$ at $V = 100$ in each layer increases to more than 50 times its value at $V = 0$. For $V = 100$ as the actuator tends to cause the substrate to bend in a direction opposite to that caused by the mechanical loading alone, the middle layer of the substrate undergoes severe transverse compression (Fig. 4). The actuator also induces transverse shear stresses in all the layers of the substrate, as shown by the distributions of $\bar{\sigma}_{xz}$ and $\bar{\sigma}_{yz}$ in Fig. 5.

Figure 6 shows the elasticity solution for maximum inplane normal stress ($\bar{\sigma}_x$) in the substrate as affected by the span to thickness ratio of the substrate without and with the prescribed electric potential distribution on the actuator surface, respectively. This figure demonstrates that as the value of s becomes smaller, the solution for a particular value of V ($V = 100$) deviates more from the solution obtained with $V = 0$. The other results are also affected in the same manner as given in Table 2.

From the foregoing analyses it is apparent that for a given value of s, and mechanical load acting on the intelligent square plate, there exists a particular voltage of actuation for which the midplane deflection is zero. Figure 7 illustrates such a value of V necessary to make the deflection of the substrate zero for a particular value of s. It is also established from the figure that the effectiveness of the actuator increases as the value of s decreases, since it is required to prescribe higher electric potential on the actuator surface as s increases. This result may be due to the fact that for a given mechanical load the stresses and deflections of a laminated plate decrease as the span to thickness ratio of the plate decreases.[4] It is also found (not shown in Fig. 7) that the value of V necessary to obtain the zero midplane deflection for very thin plate substrate (e.g., $s = 100$) is within the breakdown voltage (2000 V)[9] for PVDF.

Finally, the capability of the sensor layer to sense the deformations in terms of induced electric potential on its surface as influenced by the deformation of the substrate is shown in Figs. 8 and 9. The variation of the thickness of the sensor and actuator layers within the commercially available range[12] (9 μ to 0.5 mm) affects the elasticity solution negligibly (not presented here). But the induced electric potential on the sensor surface varies considerably, as shown in Figs. 8 and 9.

Conclusions

The exact solutions for static analysis of a simply supported rectangular plate-type intelligent structure is presented here.

The structure is composed of a laminated substrate of graphite/epoxy composite coupled with distributed sensor and actuator layers of biaxially polarized piezoelectric polymer, called PVDF. The actuator layer causes the layers of the substrate to undergo bending, transverse compression, inplane shear, and transverse shear deformations. The effectiveness of the actuator layer increases with the decrease in the length to thickness ratio of the substrate. The variation of the thickness of the piezoelectric layers within the range of 9 μ to 0.5 mm affects the elasticity solutions negligibly. But the induced electric potential on the surface of the sensor varies considerably. The procedure for the solutions can be employed to study the performance of other piezoelectric materials such as lead zirconate titanate to act as sensor and actuator. The results can be useful for the verification of the solutions obtained from further analysis of an intelligent structure of complicated geometry subjected to other boundary conditions by approximate methods.

References

[1]Ray, M. C., Rao, K. M., and Samanta, B., "Exact Analysis of Coupled Electroelastic Behavior of Piezoelectric Plate Under Cylindrical Bending," *Computers and Structures,* Vol. 45, No. 4, 1992, pp. 667–677.

[2]Ray, M. C., Rao, K. M., and Samanta, B., "Exact Solution for Static Analysis of Intelligent Structures under Cylindrical Bending," *Computers and Structures* (to be published).

[3]Ray, M. C., Rao, K. M., and Samanta, B., "Exact Solution for Static Behavior of Piezoelectric Layer Used in Intelligent Structures," Dept. of Mechanical Engineering, IIT-KGP-ESL-91-03, Indian Inst. of Technology, Kharagpur, India.

[4]Pagano, N. J., "Exact Solutions for Rectangular Bidirectional Composites and Sandwich Plates," *Journal of Composite Material,* Vol. 4, Jan. 1970, pp. 20–34.

[5]Tiersten, H. F., *Linear Piezoelectric Plate Vibration,* Plenum Press, New York, 1969.

[6]Cady, W. G., *Piezoelectricity,* McGraw-Hill, New York, 1946.

[7]Tzou, H. S., and Pandita, S., "A Multi-Purpose Dynamic and Tactile Sensor for Robot Manipulators," *Journal of Robotic System,* Vol. 4, 1987, pp. 719–741.

[8]Hoff, N. J., and Rehfield, L. W., "Buckling of Axially Compressed Circular Cylindrical Shells at Stresses Smaller than the Classical Critical Value," *Journal of Applied Mechanics,* Vol. 32, Sept. 1965, pp. 542–546.

[9]Tzou, H. S., and Tseng, C. I., "Distributed Piezoelectric Sensor/Actuator Design for Dynamic Measurement/Control of Distributed Parameter Systems: A Piezoelectric Finite Element Approach," *Journal of Sound and Vibration,* Vol. 138, No. 1, 1990, pp. 17–34.

[10]Meric, R. A., and Saigal, S., "Shape Sensitivity Analysis of Piezoelectric Structures by the Adjoint Variable Method," *AIAA Journal,* Vol. 29, No. 8, 1991, pp. 1313–1318.

[11]Crawley, E. F., Luis, J., Hagood, N. W., and Anderson, E. H., "Development of Piezoelectric Technology for Applications in Control of Intelligent Structures," *Proceedings of the American Control Conference,* June 1988.

[12]Gerliczy, G., "Piezoelectric SOLEF PVDF Polyvinylidene Fluoride Films and Sheets," Solvay Technologies, Inc., New York, 1991.